

Microrheology of Supercooled Liquids in Terms of a Continuous Time Random Walk

Carsten F. E. Schroer and Andreas Heuer

In this short note we compare the discretization of the dynamics of supercooled liquids in configuration space, using metabasins, with the discretization in real space, using a distance criterion. It turns out that several observables, such as waiting-time distributions, are rather similar. However, significant deviations are observed when applying an external force. It is argued that the configuration space discretization is somewhat superior. Reprinted with permission from J Chem. Phys. 138, 12A518 (2013). Copyright 2013, AIP Publishing LLC.”

23.1 Introduction

Since the continuous time random walk (CTRW) analysis presented in the original article requires the minimization of structures concerning their potential energy [1], it comes along with a rather high numerical effort. Therefore, the important question emerges, whether a discretization of single particle trajectories in real space is also able to offer the same spatial and temporal information as our potential energy landscape (PEL) approach.

In literature, several approaches have been reported to discretize single particle trajectories into stochastic events [2, 3, 4, 5, 6]. However, there were major differences between the used protocols, especially, concerning the distance the particles have to travel until their motion is counted as a “transition”. Furthermore, there are differences how the vibrational dynamics of the particles is treated during the analysis. While in Ref. [2], motion is separated into low displacement (i.e. vibrational) and high displacement (i.e. diffusive) events, the vibrational part has been removed in Ref. [3] and Ref. [5] via integration of the spatial distribution function [3] or rather averaging the trajectories in certain time intervals [5].

Our aim was to develop a procedure to define real space transitions which is close to the results we have obtained from our PEL analysis. Therefore, we have adopted the averaging procedure from Ref. [5] which enables a suppression of thermal vibration and provides hopping-like trajectories, similar to the athermal metabasin trajectories one obtains from the PEL analysis [1]. Since there is a large variety of possibilities for how to define a spatial threshold, it might be reasonable for a first guess to use the simplest criterion, which is that a particle travels a distance d from its present position. This kind of criterion was used, e.g. in Ref. [6]. It has been shown in Ref. [7] that the waiting-times resulting from this type of discretization can very well reproduce the basic properties of the PEL waiting-time distribution.

23.2 Computational Details

The analysis has been performed for the same binary Lennard-Jones liquids that was studied in our original article. Please note, that we have restricted our analysis to a temperature range above the computer glass transition, so that no aging behavior is expected. As a first step, the real space trajectories have been averaged over 200 structures, thus, reducing the local vibrations. Because we wanted to study the properties of a microrheologically driven system, where the motion of the tracer particle is biased by an external force F , we had to slightly modify the criterion for the definition of an event: We count a transition to occur when the tracer particle either moves a distance $+d$ *along* or a distance $-d$ *against* the force direction. If an event has taken places, the current position of the tracer particle is defined as the starting point for the next transition. The local waiting-time τ^{local} is defined as the time between two of these events. Please note, that we have not counted the time from the beginning of the simulation to the first event, so our τ^{local} is related to the exchange times in Ref. [6]. The computed local waiting-times strongly depend on the chosen local threshold d . To be as close as possible to the metabasin analysis we chose a value for $d = 0.01$ for which we recover a distribution of local waiting-times $\varphi(\tau^{\text{local}})$ which is, independent from temperature, in good agreement with the distribution of metabasin waiting-times $\varphi(\tau^{\text{MB}})$ for $F = 0$ (see Fig. 23.1).

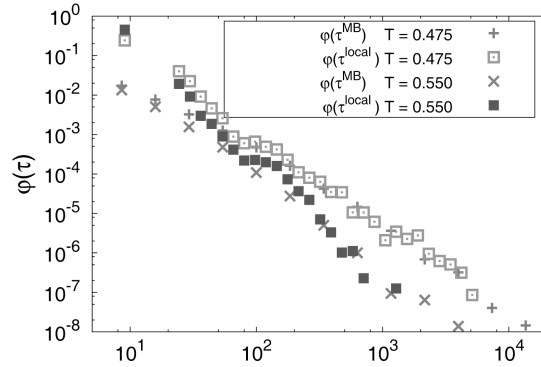


Figure 23.1: Distribution of local (crosses) and metabasin (squares) waiting-times for $T = 0.475$ and $T = 0.55$ and no applied force.

23.3 Results

One of the central quantities we have studied in the original article was the long-time velocity \bar{v} of the tracer particle parallel to the force direction

$$\bar{v} = \lim_{t \rightarrow \infty} \frac{x_{\parallel}(t) - x_{\parallel}(t_0)}{t - t_0} \quad (23.1)$$

where x_{\parallel} denotes the absolute position of the tracer particle along the force axis. By discretizing the trajectory of the tracer particle into single events, \bar{v} decomposes into a spatial part $\langle \Delta x_{\parallel} \rangle$ and a temporal part $\langle \tau \rangle$

$$\bar{v} = \frac{\langle \Delta x_{\parallel} \rangle}{\langle \tau \rangle} \quad (23.2)$$

where $\langle \dots \rangle$ denotes an average over a large number of single events. In our original article we have identified $\langle \Delta x_{\parallel} \rangle$ with the average displacement of the tracer particle parallel to the force direction during one metabasin transition and $\langle \tau \rangle$ with the average metabasin waiting-time. In the following we will write $\langle \Delta x_{\parallel}^{\text{MB}} \rangle$ or rather $\langle \tau^{\text{MB}} \rangle$ if we refer to the quantities resulting from the MB discretization.

For the local events one can also obtain the spatial and temporal quantities of Eq. 23.2, however, there are some qualitative differences. While the temporal part results from a distribution function $\varphi(\tau^{\text{local}})$ which is, at least without an applied force, similar to the metabasin distribution (see Fig. 23.1), the spatial part is obtained by

$$\langle \Delta x_{\parallel}^{\text{local}} \rangle = d \cdot \frac{\# \text{Events}(+) - \# \text{Events}(-)}{\# \text{Events}(+) + \# \text{Events}(-)} \quad (23.3)$$

where $\# \text{Events}(+)$ denotes the number of events along, $\# \text{Events}(-)$ the number of events against the force direction and d the chosen radius (compare

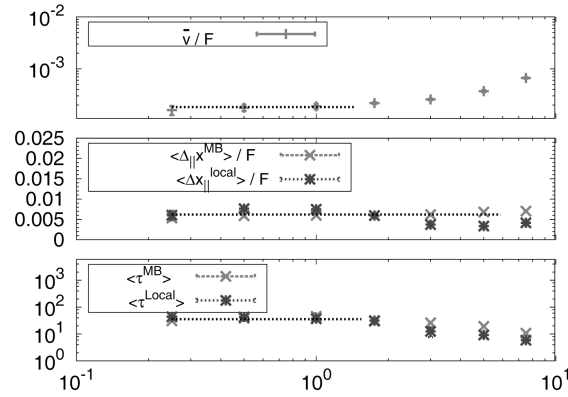


Figure 23.2: *Upper panel.* Drift velocity \bar{v} divided by force F at $T = 0.475$. The dashed line indicates the linear response regime up to a the critical force $F_{c,v}$ (see text). *Middle panel.* Average spatial displacements $\langle \Delta x_{\parallel}^{\text{MB}} \rangle$ and $\langle \Delta x_{\parallel}^{\text{local}} \rangle$ divided by force F at $T = 0.475$. The dashed line indicates the linear response regime up to a the critical force $F_{c,\Delta x}$ (see text). *Lower panel.* Average waiting times $\langle \tau^{\text{MB}} \rangle$ and $\langle \tau^{\text{local}} \rangle$ at $T = 0.475$. The dashed line indicates the linear response regime up to a the critical force $F_{c,\frac{1}{\tau}}$ (see text).

Sec. 23.2). This means, that in contrast to the MB quantity, $\langle \Delta x_{\parallel}^{\text{local}} \rangle$ results from a bimodal distribution and is restricted to a range of $[-d, +d]$. This also means, that the choice of d also determines the outcome of the analysis, however, since $\varphi(\tau^{\text{local}})$ is close to $\varphi(\tau^{\text{MB}})$ (see Fig. 23.1) and Eq. 23.2 is valid, also the average $\langle \Delta x_{\parallel}^{\text{local}} \rangle$ must be close to $\langle \Delta x_{\parallel}^{\text{MB}} \rangle$.

The resulting average values are shown in Fig. 23.2. For $\langle \Delta x_{\parallel}^{\text{MB}} \rangle$ and $\langle \tau^{\text{MB}} \rangle$ one observes the interesting fact that linear and nonlinear response are nearly exclusively decomposed: while $\langle \Delta x_{\parallel}^{\text{MB}} \rangle$ stays linear for almost the whole range of forces, $\langle \tau^{\text{MB}} \rangle$ is constant for very low forces and displays a decay at intermediate forces. As it can be observed in comparison to the upper panel of Fig. 23.2, this decay coincides with the onset of nonlinear behavior of the velocity \bar{v} . This behavior becomes more obvious by comparing the critical forces $F_{c,X}$ at which the dynamical response of quantity X differ more than 10% from the expected linear response value: While $F_{c,\frac{1}{\tau}}$ and $F_{c,v}$ are identical, $F_{c,\Delta x}$ differs about a factor of three from this value.

For the average values resulting from the real space discretization, the situation appears different. Although one also notice a relation between the linear response and the spatial part, there is no hint to apportion the nonlinear response only to $\langle \tau^{\text{local}} \rangle$. At the force where one observes a decay of $\langle \tau^{\text{local}} \rangle$, one finds a similar decay of $\langle \Delta x_{\parallel}^{\text{local}} \rangle / F$ as well. The full decomposition of linear and nonlinear response which we have broadly discussed in our original article can, therefore, not be reproduced by the local discretization.

This result is some kind off drawback because it suggests that studying the onset of nonlinearity in driven systems requires, by using the depicted protocol,

the analysis of both, spatial and temporal contributions. For the metabasin analysis indeed, only the study of the temporal part seems sufficient, which can be directly linked to the properties of the underlying PEL.

23.4 Conclusion

In this article we tried to prove, whether it is possible to regain the results of the metabasin analysis performed in “Microrheology of supercooled liquids in terms of a continuous time random walk” by applying a real space discretization procedure. The procedure was inspired by previous work in literature and turned out to recover reasonable results for equilibrium systems [7]. In contrast to undriven systems it turns out, that the real space discretization applied on microrheologically driven systems offers not identical result but unfortunately cannot recover the decomposition of linear and nonlinear contributions. On the other hand this observation emphasizes, that the results which can be obtained by our PEL approach do not just recover trivial effects one could also gain with any arbitrary protocol but allows one a different perspective on the physics of driven glassy systems.

Acknowledgements

This work was supported by DFG Research Unit 1394 “Nonlinear Response to Probe Vitrification”. Furthermore, C. F. E. Schroer thanks the NRW Graduate School of Chemistry for funding and C. Rehwald and O. Rubner for many helpful discussions about this work.

References

- [1] B. Doliwa and A. Heuer, *Phys. Rev. E* **67** 030501 (2003).
- [2] G. Wahnström, *Phys. Rev. A* **44** 3752 (1991).
- [3] H. Miyagawa and Y. Hiwatari, *Phys. Rev. A* **44** 8278 (1991).
- [4] H. Teichler, *Defect Diffus. Forum* **717** 143 (1997).
- [5] K. Vollmayr-Lee, *J. Chem. Phys.* **121** 4781 (2004).
- [6] L. O. Hedges, L. Maibaum, D. Chandler and J. P. Garrahan, *J. Chem. Phys.* **127** 211101 (2007).
- [7] C. Rehwald, O. Rubner and A. Heuer, *Phys. Rev. Lett.* **105** 117801 (2010).

Reprint 23-1: Microrheology of Supercooled Liquids in Terms of a Continuous Time Random Walk

C. F. E. Schroer and A. Heuer

J. Chem. Phys., 138, 12A518 (2013)

Reprinted with permission from AIP Publishing LLC,
Copyright 2013.

Microrheology of supercooled liquids in terms of a continuous time random walk

Carsten F. E. Schroer^{1,2,a)} and Andreas Heuer^{1,2,b)}

¹Westfälische Wilhelms-Universität Münster, Institut für Physikalische Chemie, Corrensstraße 28/30, 48149 Münster, Germany

²NRW Graduate School of Chemistry, Wilhelm-Klemm-Straße 10, 48149 Münster, Germany

(Received 2 October 2012; accepted 4 December 2012; published online 3 January 2013)

Molecular dynamics simulations of a glass-forming model system are performed under application of a microrheological perturbation on a tagged particle. The trajectory of that particle is studied in its underlying potential energy landscape. Discretization of the configuration space is achieved via a metabasin analysis. The linear and nonlinear responses of drift and diffusive behavior can be interpreted and analyzed in terms of a continuous time random walk. In this way, the physical origin of linear and nonlinear response can be identified. Critical forces are determined and compared with predictions from literature. © 2013 American Institute of Physics. [http://dx.doi.org/10.1063/1.4772627]

I. INTRODUCTION

In microrheological experiments, a physical system is brought out of equilibrium by a rather simple perturbation, which is acting on a small fraction of its constituents.¹ These experiments are of specific interest because the application of a well-defined perturbation allows, first, to give predictions about the non-equilibrium behavior of the system and, second, to gain additional information about the equilibrium properties of the system by analyzing the transition to the non-equilibrium state.

In supercooled liquids in its (quasi-)equilibrium state, one can observe a lot of unique dynamical properties such as non-exponential relaxation or violation of the Stokes-Einstein relation.² Typically, this is interpreted in terms of the presence of dynamic heterogeneities; see Ref. 3 and references therein. In recent years also, the microrheological properties of supercooled liquids have been studied experimentally^{4,5} as well as theoretically.⁶⁻⁹ The occurrence of a nonlinear dynamical response was reported for different dynamical quantities. As expected for general grounds,⁷ the nonlinear response strongly increases at lower temperatures.

For the equilibrium dynamics of supercooled liquids, it has been shown that a description of the dynamics in terms of transitions between metabasins (MB) yields important additional information about the nature of the slow dynamics at low temperatures.¹⁰⁻¹² It has been shown that this discrete dynamics fulfills all criteria of a continuous time random walk (CTRW)^{13,14} if applied to the description of a small system ($O(10^2)$ particles). Most importantly, it turns out that the diffusivity of a small system only shows very small finite-size effects¹⁵ whereas the structural relaxation time displays large effects. This can be interpreted via facilitation effects.¹⁵ Going down in temperature may in principle modify the spatial and the temporal aspects of the CTRW. Interestingly, it turns out that the slowing down at low temperatures is exclusively

determined by the temporal contributions.¹¹ Furthermore one can, for example, express the complete wave vector dependence of the structural relaxation part of the incoherent scattering function in terms of the properties of the waiting time distribution, characterizing the CTRW.¹⁴ Thus, the mapping of the MB dynamics on the CTRW is a powerful concept for the description of supercooled liquids. Unfortunately, the latter approach can be only used for small systems.³ The qualitative reason is that very large systems can be decomposed into basically independent smaller systems.¹⁵ Thus, spatial information about the dynamic processes becomes essential, which however, is not available in configuration space. More formal arguments can be found in Ref. 3.

On a qualitative level, the external force gives rise to a tilting of the potential energy landscape (PEL) for the tagged particle. The key goal of the present work is to show how the CTRW properties are modified upon this tilting. This allows us to characterize the onset of nonlinearity in the mobility of the tracer particles in terms of specific CTRW properties. Furthermore, it will be demonstrated that a small system, analogous to the equilibrium case, only displays small finite size effects, even in a highly nonlinear regime. Therefore, a closer understanding of microrheological effects in small systems allows us to unravel the underlying physics of large systems as well.

The paper is organized as follows: in Sec. II, we describe details of the simulation. Section III contains the results and their discussion. We conclude in Sec. IV.

II. SIMULATIONS

We present the results of molecular dynamics (MD) simulations of a binary Lennard-Jones mixture, which consists of two types of particles, A and B, whereas 80% of the particles are of type A. This system is known to be a prototype of a glass-forming system.¹⁶ To be able to simulate system sizes as small as 65 particles, the cutoff radius is reduced to 1.8 rather than 2.5 (in dimensionless LJ-units).¹⁷ A microrheological

^{a)}Electronic mail: c.schroer@uni-muenster.de.

^{b)}Electronic mail: andheuer@uni-muenster.de.

perturbation is introduced to the system by randomly selecting one A type particle and pulling it with a constant force F along a certain direction. To ensure that the system resides in a stationary state, the system is equilibrated under application of the force to the tracer particle. *A priori* it might be questionable, whether this equilibration procedure leads to different results than equilibrating the system without the force and starting the application at the beginning of the simulation. To investigate this, we have performed additional simulations in which the external field is switched off during the equilibration time.

A constant temperature during our simulations is achieved by coupling the system to a Nosé-Hoover thermostat.¹⁸ To avoid an unphysical cooling of the bath particles, the tracer particle is excluded from the thermostat. For each temperature and force pair, we performed 15 to 30 independent simulations.

A key element of our analysis is the tracking of minima of the PEL, which the system explores during its time evolution and which displays the impact of the external force. We access these minimum energy structures by applying a suitable optimization algorithm¹⁷ on the particle's coordinates with respect to their potential energy. Furthermore, following the procedure as outlined in Refs. 3 and 17, the minima are grouped together to metabasins (MB). As mentioned above, the potential energy is minimized for the complete potential energy, including the effect of the external force. In practice, it turns out that for somewhat larger forces ($F > 10$) the minimization routine becomes unstable. In any event, no larger forces are needed since the onset of nonlinear effects occurs at much smaller values of F .

In MD simulations, one generally prefers to simulate systems as large as possible to avoid any unphysical behavior due to the finite-size of the system. However, since the CTRW approach in configuration space is only valid for small system sizes,³ we focus on a small system with $N = 65$ (BLJM65), which is close to the smallest system size without significant finite-size effects for the diffusivity.¹⁹ Due to linear response theory, this automatically implies that also the linear regime of the mobility in the microrheological setup should not display relevant finite-size effects. Whether or not this holds also for the nonlinear regime will be checked by comparison with the simulations of a larger system with 1560 particles and a geometry of 3 : 1 : 1, the long side pointing along the force direction (BLJM1560).

III. RESULTS AND DISCUSSION

A. Drift velocity in real space

One central quantity in the analysis of microrheological properties is the drift velocity v the tracer particle obtains due to the interplay of permanent acceleration along the force direction and friction effects. Formally, the drift velocity is given by the stationary long-time limit of the displacement of the tracer particle parallel to the force direction $x_{\parallel}(t)$ relative to the time.

$$v = \lim_{t \rightarrow \infty} \frac{x_{\parallel}(t) - x_{\parallel}(t_0)}{t - t_0}. \quad (1)$$

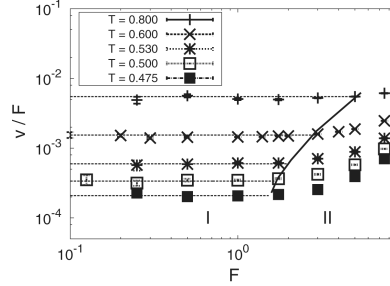


FIG. 1. Drift velocity v of BLJM65. The dashed lines correspond to the expected linear response behavior (see Eq. (2)). The solid line indicates the critical forces $F_{c,v}$ at which the linear response regime (I) transforms into the nonlinear regime (II) (see Eq. (4)).

For BLJM65, the force dependence of the drift velocity for different temperatures is shown in Fig. 1. In the range of forces of our investigation, one can observe two regimes: a low force regime (I) in which the velocity increases linearly with increasing force and a high force regime (II) in which it exhibits a nonlinear growth of velocity.

In the first regime, the velocity satisfies the linear response relation

$$v = D_0 \beta F, \quad (2)$$

(dashed lines in Fig. 1) in which D_0 stands for the one-dimensional diffusion constant in equilibrium and $\beta = \frac{1}{k_B T}$ for the inverse thermal energy. It is of particular interest that the size of the linear regime is temperature dependent so that it decreases with decreasing temperature. Similar to the work of Williams *et al.*,⁷ we quantify this observation by fitting the curves with a symmetric power law

$$\frac{v}{F} = a_2 F^2 + a_0. \quad (3)$$

Using this fit, one can define a threshold force

$$F_{c,v} = \sqrt{\frac{0.1 a_0}{a_2}} \quad (4)$$

by the criterion that the dynamical response differs more than 10% from the expected linear response behavior. The values of these threshold forces are indicated as solid lines in Fig. 1. The critical forces are further discussed in Sec. III D.

To analyze possible finite-size effects for the velocity, we have compared the drift velocity of the BLJM65 and BLJM1560 at a temperature of $T = 0.475$. In the linear regime, one observes that the velocity of the larger system slightly differs from the small system. According to linear response theory, this just reflects analogous effects for the equilibrium diffusivity as reported in Ref. 15. Additional differences of the equilibrium diffusivities can result from hydrodynamic effects due to the different geometries. Most interestingly, after superimposing the velocity of the systems in the linear regime (see Fig. 2) also the results for the nonlinear regimes are rather close. Especially, the onset of nonlinear

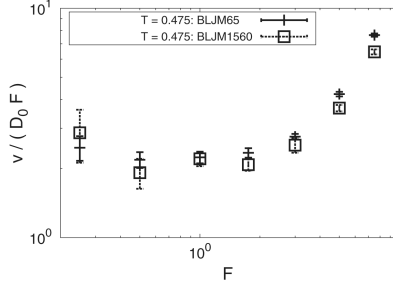


FIG. 2. Drift velocity v for BLJM65 and BLJM1560 at a temperature $T = 0.475$. v was normalized via the particular equilibrium diffusion constants D_0 .

effects seems to be equal for both system sizes. Thus, understanding the nonlinearity for BLJM65 is sufficient to unravel the underlying physics also of large systems. In particular, this allows one to use the CTRW framework in configuration space for the elucidation of microrheological effects.

Another type of finite-size effect might result from the equilibration of the system under application of the force. To elucidate this, we have compared the drift velocities of the tracer particle in a system, which was equilibrated with and without the applied force field. The results are shown in Fig. 3. For the switch-on experiment, one observes that the drift velocity reaches a steady-state at $t \approx 500$. The velocities of these steady-states are identical to the velocities we have determined from the simulations, which were equilibrated within the applied field. The time window which is shown in Fig. 3 is lower than the expected time t_{pass} the particle needs to travel through the simulation box (for $F = 5$: $t_{pass} = 1309$).

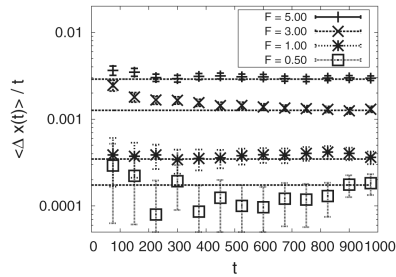


FIG. 3. Average displacement $\langle \Delta x(t) \rangle$ of the tracer particle along the force direction for BLJM65 at $T = 0.5$. The data points correspond to a system, which was equilibrated without the application of the external force. The dashed lines indicate the average velocity v of the system, which was equilibrated under application of the forcefield.

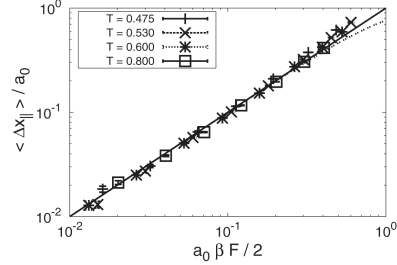


FIG. 4. Average displacement of the tracer particle during one MB transition $\langle \Delta x_{\parallel} \rangle$ as a function of the applied force F . The solid line indicates the linear response prediction by Eq. (8) while the dashed line includes the theoretical prediction of nonlinear effects (Eq. (9)).

B. Drift velocity in CTRW terms

In principle, any kind of discretization of the trajectories allows the decomposition of dynamical quantities in a spatial and a temporal part. In case of the drift velocity, one can generally write

$$v = \frac{\langle \Delta x_{\parallel} \rangle}{\langle \tau \rangle}. \quad (5)$$

This relates the long-time drift to the average displacement of the tracer particle along the force direction during a single elementary step, $\langle \Delta x_{\parallel} \rangle$ and the average waiting time $\langle \tau \rangle$. Because the waiting time cannot be affected by the direction of the applied force, the value of $\langle \tau \rangle$ can only depend on even powers of F . Therefore, the linear response regime of small forces has to be related to the force dependence of the spatial part. However, in case of the nonlinear regime, it is *a priori* not clear, whether the spatial or temporal effects dominate the dynamical responses.

The force dependence of $\langle \Delta x_{\parallel} \rangle$ is shown in Fig. 4. One observes a linear scaling at low and intermediate forces. This behavior can be quantitatively understood by taking into account that the equilibrium diffusion constant D_0 can be expressed in CTRW terms¹¹ as

$$D_0 = \frac{a_0^2}{2\langle \tau \rangle}. \quad (6)$$

The length scale a_0^2 refers to the one-dimensional averaged diffusive length, a single A type particle moves during one MB transition in an equilibrium system. It is defined by the single particle displacement x in one dimension after a large number of transitions n via

$$a_0^2 = \lim_{n \rightarrow \infty} \frac{\langle (x(n) - x(0))^2 \rangle}{n}. \quad (7)$$

As it was discussed in Ref. 11, a_0^2 is a temperature independent quantity. Inserting Eqs. (5) and (6) in Eq. (2), one obtains for the linear response regime

$$\langle \Delta x_{\parallel} \rangle = \frac{a_0^2}{2} \beta F, \quad (8)$$

which is indicated as a solid line in Fig. 4.

For the evolution of $\langle \Delta x_{\parallel} \rangle$ in the nonlinear regime, one can make a prediction by considering a one-dimensional periodic potential with a constant distance a_0 between two adjacent minima. Under application of the force, the jumping directions become biased so that one gets for the average displacement

$$\langle \Delta x_{\parallel} \rangle = a_0 \tanh \frac{a_0}{2} \beta F. \quad (9)$$

This particular ansatz was further discussed by Jack *et al.*²⁰ By linear expansion, Eq. (9) also includes the linear response relation (Eq. (8)). However, from Eq. (9) one would expect a negative nonlinear response because the F^3 term of the expansion has a negative sign. In contrast, our numerical results display a slightly positive $O(F^3)$ term. One can qualitatively understand this behavior by taking into account that in the theoretical ansatz a_0 is regarded as a force independent quantity. Especially at higher forces, one could expect that the diffusive length increases with increasing force as well (see also below). Unfortunately, one cannot immediately identify a specific length, which displays the expected behavior to quantitatively reproduce the nonlinear growth of the particle displacement. Thus, we see that the spatial aspects of the hopping behavior at large forces cannot be described by this simple approach of equidistant minima.

In any event, the key conclusion from this analysis is the smallness of the nonlinear increase. Even at the lowest temperature and highest force, it is smaller than a factor of 1.25. As a conclusion, the spatial part of the drift velocity comes with a distinct linear and a very weak nonlinear response.

Concerning the temporal part, we show the waiting time distribution $\varphi(\tau)$ in Fig. 5. In the case of small forces, the distribution of waiting times does not change so that the curves collapse as expected for the linear response regime. Indeed, in case of higher forces, long waiting times do not occur any more so that the distribution functions decay faster. This has major consequences for the average waiting time $\langle \tau \rangle$ (see Fig. 6): while for small forces, $\langle \tau \rangle$ stays constant, one can observe a drop for forces higher than a critical force. We characterize the critical behavior of the temporal part by determining the critical force of the inverse average waiting time $1/\langle \tau \rangle$,

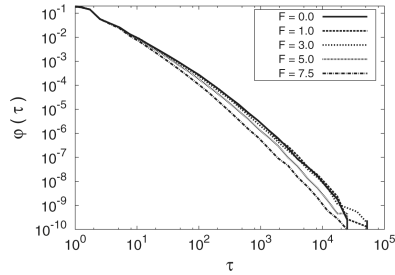


FIG. 5. Distribution of MB waiting times τ during one MB transition at a temperature $T = 0.475$.

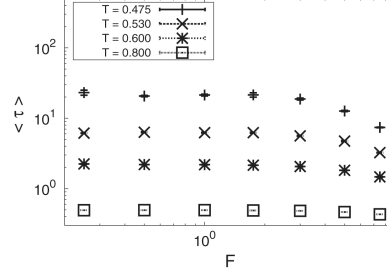


FIG. 6. Average waiting times $\langle \tau \rangle$ as a function of external forces F .

which is the relevant contribution to the drift velocity (see Eq. (5)). It turns out, that the critical force $F_{c,\perp}$ is identical to $F_{c,v}$. This fact underlines the major influence of the temporal part to the nonlinear behavior of the drift velocity. For further discussion in Sec. III D, we will thus not distinguish between these critical forces and restrict our analysis on $F_{c,\perp}$.

The transition to the nonlinear regime of v can be regarded as a direct consequence of the nonlinear behavior of $\langle \tau \rangle$. The observations of the different force dependencies of the spatial and the temporal part interestingly illustrate that the discretization of the trajectory in the MB approach also leads to a decomposition of linear and nonlinear contributions to the drift velocity: In case of small forces, $\langle \tau \rangle$ stays constant so that the linear response can be completely related to the spatial part. The nonlinear regime, however, is governed by a decay of the average waiting time.

On a qualitative level, this picture agrees with the idea of linear response theory as applied to a simple 1D cosine-potential. Naturally, $\langle \Delta x_{\parallel} \rangle$ is proportional to the force in the linear regime. Thus, any variation of the waiting times, e.g., to a modification of the barriers, gives rise to higher-order effects in the resulting mobility. Stated differently, the nonlinearity mainly reflects the modification of the underlying PEL upon application of a large external force.

C. Diffusion in CTRW terms

As it was already mentioned above (see Eq. (6)), the one-dimensional diffusion constant in equilibrium of a single particle is given in CTRW terms as the ratio of the isotropic diffusive length a_0^2 and the average waiting time $\langle \tau \rangle$. Going towards driven system, one has to distinguish between the diffusive processes parallel and perpendicular to the force direction, which were characterized by the diffusion constants D_{\parallel} and D_{\perp} , respectively. Because $\langle \tau \rangle$ is a universal quantity, expected differences between parallel and perpendicular diffusion are related to the anisotropy of the respective length scales. In analogy to Eq. (7), we define the length scale in perpendicular direction a_{\perp}^2 as

$$a_{\perp}^2 = \lim_{n \rightarrow \infty} \frac{\langle (x_{\perp}(n) - x_{\perp}(0))^2 \rangle}{n} \quad (10)$$

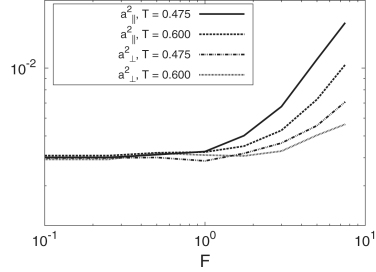


FIG. 7. Diffusive length scales a_{\parallel}^2 (two upper lines) and a_{\perp}^2 (two lower lines) of the tracer particle parallel and perpendicular to the force direction as a function of the external force F .

and the parallel length scale a_{\parallel}^2 as

$$a_{\parallel}^2 = \lim_{n \rightarrow \infty} \frac{(\langle x_{\parallel}(n) - x_{\parallel}(0) \rangle^2)}{n} - \langle \Delta x_{\parallel} \rangle^2. \quad (11)$$

Please note that in the latter definition, the systematic drift of the tracer particle along the force direction was subtracted. The corresponding length scales are shown in Fig. 7. One can observe that both, a_{\parallel}^2 and a_{\perp}^2 , exhibit an increase with increasing force, which is stronger for the parallel direction. Interestingly, although a_{\perp}^2 and a_{\parallel}^2 are temperature independent in equilibrium, corresponding to the linear regime, the degree of nonlinearity strongly depends on temperature. As already indicated above, one may expect that the PEL properties change in the nonlinear regime. Since these modifications are expected to be strongly anisotropic, it is not surprising that observables, defined parallel or orthogonal to the applied force, may behave differently.

Dividing a_{\parallel}^2 and a_{\perp}^2 by $2\langle \tau \rangle$ one obtains the parallel and the orthogonal diffusion constants D_{\parallel} and D_{\perp} , respectively. Since the denominator is always the same, the different increase of a_{\parallel}^2 as compared to a_{\perp}^2 directly translates into the corresponding relative increase of D_{\parallel} as compared to D_{\perp} . Furthermore, the weak force dependence of $\langle \Delta x_{\parallel} \rangle$ directly translates into a weaker force dependence of the mobility as compared to both diffusion constants. Actually, the observed relation $D_{\parallel} \gg D_{\perp} > \frac{v}{\beta F}$ (see Fig. 8) was already reported for the lithium dynamics in a lithium silicate system.²¹ This suggests that the force dependent anisotropy of the relevant length scales is a general property of disordered systems.

The diffusion constant D_{\perp} can also be measured by fitting the slope of the long-time limit of the mean-squared displacement $\langle x_{\perp}^2(t) \rangle$ perpendicular to the force direction. Indeed, this is not possible for D_{\parallel} because there one observes superdiffusive behavior for intermediate times, as it was also reported in Ref. 9, and diffusive behavior with a much higher diffusion constant for long times, as it was predicted in Ref. 20, especially when a strong force is applied. The origin of this anomalous behavior can be traced back to the existence of dynamical heterogeneities, and can be quantitatively understood in terms of the presented CTRW approach.²² In that frame-

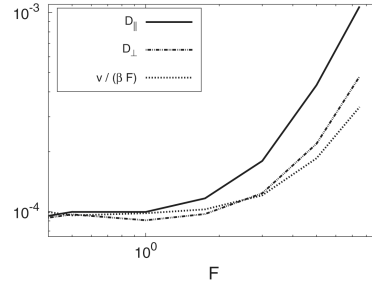


FIG. 8. Nonlinear responses of the diffusion coefficients parallel (D_{\parallel}) and perpendicular (D_{\perp}) to the force direction and of the drift velocity v at a temperature $T = 0.475$.

work, D_{\parallel} describes the underlying diffusive processes, which is superimposed by superdiffusive contributions.

D. Critical forces

Finally, it is of interest to compare the nonlinear response of the different observables on a more quantitative level. Since we are mainly interested in the onset of nonlinearity, an appropriate measure is the critical force as introduced in Eq. (4). Here, we concentrate on a_{\parallel}^2 , a_{\perp}^2 , and $1/\langle \tau \rangle$ as the key observables of the CTRW approach. The remaining variable $\langle \Delta x_{\parallel} \rangle$ is omitted because its nonlinearity is extremely small. Furthermore, the critical force of the drift velocity $F_{c,v}$ is not discussed separately because, as it was mentioned above, it has been found to be identical with $F_{c,\perp}$.

In Fig. 9, all critical forces are shown as a function of temperature. It can be seen that in general for a given temperature each observable has a different critical force. Furthermore, the temperature dependence varies quite significantly. Whereas for the length scales the critical forces scale

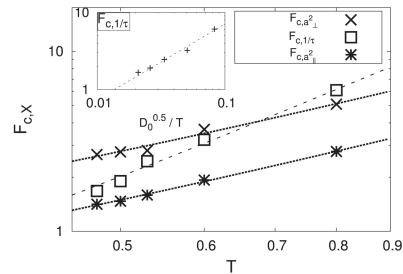


FIG. 9. Critical forces $F_{c,X}$ of different dynamical quantities $X = a_{\parallel}^2$, a_{\perp}^2 , and $\frac{1}{\tau}$. The dashed lines indicate a behavior $F_{c,X} \propto T^{1.5}$ or rather $F_{c,X} \propto T^{2.5}$. Inset: $F_{c,\perp}$ as a function of $\sqrt{\frac{D_0}{T}}$ with the equilibrium diffusion constant D_0 . The dashed line indicates a linear behavior.

similarly to $F_{c,x} \propto T^{1.5}$, the critical force of the inverse waiting time roughly scales like $F_{c,\perp} \propto T^{2.5}$.

A theoretical prediction about the onset of nonlinearity can be found in Ref. 23. It was suggested by the authors that linear response relation of the time-averaged dissipative flux \bar{v} in a driven system holds exactly when the steady state fluctuation theorem

$$\lim_{t \rightarrow \infty} \frac{p(\bar{v} = A)}{p(\bar{v} = -A)} = \exp(A\beta Ft) \quad (12)$$

is fulfilled. From this condition, the scaling

$$F_{c,v} \propto \frac{\sqrt{D_0}}{T} \quad (13)$$

has been derived in which D_0 stands for the equilibrium diffusion coefficient.⁷ In the inset of Fig. 9, one can observe that $F_{c,\perp}$, and therefore naturally $F_{c,v}$ as well, fulfills the scaling prediction.

IV. CONCLUSION

In the present paper, we have analyzed the dynamics of a driven single particle in a supercooled liquid in terms of a CTRW. In case of the drift velocity, the discretization of the MB approach allows one to identify the temporal part of the CTRW as the key source of non linear response, whereas the spatial part only exhibits a weak positive contribution. This positive contribution can be qualitatively understood by the fact that the distances between adjacent MB increase due to the application of higher forces. Since the finite-size effects are small these results also reflect the origin of the nonlinear response in the much larger system.

In terms of a CTRW analysis, we have been able to determine the relevant diffusive lengths of the tracer particle diffusion along the directions parallel and perpendicular to the force. Among others, this enables the definition of a parallel diffusion constant, which is not directly accessible from real space trajectories.⁹

The force dependencies of parallel diffusion, perpendicular diffusion, and drift velocity are significantly different. Thus, there is no general critical force, which designates a mutual transition to a nonlinear regime. However, in terms of dynamical quantities, one can regard the critical force of the inverse waiting time as a key entity because of its relation to the velocity (neglecting the minor nonlinear effects of the spa-

tial part). For this quantity, one also observes the validity of the theoretical scaling prediction by Evans *et al.*²³

This observation is of major conceptual interest because the theoretical prediction is based on steady state fluctuation arguments while the CTRW waiting time is determined by the underlying PEL, i.e., by the distribution of minimum energies and saddle heights as well as the topography. Because the waiting time decreases under the application of the external force, one can assume that the force dependence of at least one of these distributions is responsible for this behavior. It remains to be shown which specific variations of the PEL give to the transition for linear to nonlinear dynamics.

ACKNOWLEDGMENTS

This work was supported by the DFG Research Unit 1394 “Nonlinear Response to Probe Vitrification.” Furthermore, C. F. E. Schroer thanks the NRW Graduate School of Chemistry for funding and C. Rehwald and O. Rubner for many helpful discussions about this work.

- ¹P. Cicuta and A. M. Donald, *Soft Matter* **3**, 1449 (2007).
- ²K. Binder and W. Kob, *Glassy Materials and Disordered Solids: An Introduction to Their Statistical Mechanics* (World Scientific, 2005).
- ³A. Heuer, *J. Phys.: Condens. Matter* **20**, 373101 (2008).
- ⁴P. Habdas, D. Schaar, A. C. Levitt, and E. R. Weeks, *Europhys. Lett.* **67**, 477 (2004).
- ⁵L. G. Wilson, A. W. Harrison, A. B. Schofield, J. Arlt, and W. C. K. Poon, *J. Phys. Chem. B* **113**, 3806 (2009).
- ⁶C. Reichhardt and C. J. O. Reichhardt, *Phys. Rev. E* **74**, 011403 (2006).
- ⁷S. R. Williams and D. J. Evans, *Phys. Rev. Lett.* **96**, 015701 (2006).
- ⁸I. Gazuz, A. M. Puertas, T. Voigtmann, and M. Fuchs, *Phys. Rev. Lett.* **102**, 248302 (2009).
- ⁹D. Winter, J. Horbach, P. Virnau, and K. Binder, *Phys. Rev. Lett.* **108**, 028303 (2012).
- ¹⁰F. H. Stillinger, *Science* **267**, 1935 (1995).
- ¹¹B. Doliwa and A. Heuer, *Phys. Rev. E* **67**, 030501 (2003).
- ¹²V. K. de Souza and D. J. Wales, *J. Chem. Phys.* **129**, 164507 (2008).
- ¹³L. Berthier, D. Chandler, and J. P. Garrahan, *EPL* **69**, 320 (2005).
- ¹⁴O. Rubner and A. Heuer, *Phys. Rev. E* **78**, 011504 (2008).
- ¹⁵C. Rehwald, O. Rubner, and A. Heuer, *Phys. Rev. Lett.* **105**, 117801 (2010).
- ¹⁶W. Kob and H. C. Andersen, *Phys. Rev. E* **51**, 4626 (1995).
- ¹⁷B. Doliwa and A. Heuer, *Phys. Rev. E* **67**, 031506 (2003).
- ¹⁸S. Nosé, *J. Chem. Phys.* **81**, 511 (1984).
- ¹⁹S. Büchner and A. Heuer, *Phys. Rev. E* **60**, 6507 (1999).
- ²⁰R. L. Jack, D. Kelsey, J. P. Garrahan, and D. Chandler, *Phys. Rev. E* **78**, 011506 (2008).
- ²¹M. Kunow and A. Heuer, *J. Chem. Phys.* **124**, 214703 (2006).
- ²²C. F. E. Schroer and A. Heuer, “Anomalous diffusion of driven particles in supercooled liquids,” arXiv:1210.1081.
- ²³D. J. Evans, D. J. Searles, and L. Rodoni, *Phys. Rev. E* **71**, 056120 (2005).